DTU Library

# Hygrothermal conditions in the facades of residential buildings in Nuuk and Sisimiut

**Friis, Naja Kastrup; Møller, Eva B.; Lading, Tove**

*Published in:*
Building and Environment

*Link to article, DOI:*
10.1016/j.buildenv.2023.110686

*Publication date:*
2023

*Document Version*
Publisher's PDF, also known as Version of record

Building and Environment 243 (2023) 110686

Contents lists available at ScienceDirect

Building and Environment

journal homepage: www.elsevier.com/locate/buildenv

# Hygrothermal conditions in the facades of residential buildings in Nuuk and Sisimiut

Naja Kastrup Friis *, Eva B. Møller, Tove Lading

*Technical University of Denmark, Brovej 118, 2800, Kgs. Lyngby, Denmark*

ARTICLE INFO

*Keywords:*
Hygrothermal simulations
Arctic climate
Measurements
Façade constructions
Mould index
Membranes

ABSTRACT

The limited documentation of the performance of previous and present building techniques in Greenland confines the basis for optimal design decisions. This study presents hygrothermal data from nine houses in Nuuk and Sisimiut, representing constructions of half-timber, concrete, and cross-laminated timber, all designed with a ventilated air cavity. The temperatures and relative humidity are monitored on the wall's inner side, in the air cavities and on each side of possible implemented wind and vapour membranes. The data are subjected to intercomparisons and compared to simulations from the hygrothermal simulation tool, Delphin. Finally, the measured and simulated data are analysed for the risk of mould growth with the Viitanen model in the free software WUFI Mould Index VTT. It is found that all construction types can function adequately under Greenlandic conditions. It is, however, recommended to be critical when excluding building elements, such as wind barriers, due to the risk of reduced performance of the façade structure. Furthermore, it is found that the mould risk is minimal inside the constructions but to some extent critical in the air cavities; however, the consequences of mould there are limited. Finally, the results are compared to other similar studies.

## 1. Introduction

### *1.1. Greenlandic history and building tradition*

The construction industry in Greenland has been under rapid development in the last 150 years. Traditionally, people lived in smaller communities and settlements, and even up to the middle of the 19th century, some people lived in peat houses [1]. Originally, the Greenlandic people lived as nomads until the missionaries and the traders began to see advantages in stationary trading posts. This interference caused a change in the way of living, building, and organising society [1]. Since the development of the Greenlandic Technical Organisation (GTO) in 1950, the architectural style has been everchanging, from small wooden standard houses to multistorey concrete buildings [2]. Unfortunately, the evaluation of the implemented building methods has been irregular and inadequate, causing gaps in the knowledge regarding proper building methods in Greenland. When constantly implementing new design solutions on multiple buildings before evaluating the performance, the consequences can be costly, e.g., due to reduced service life, increased heating demand, or extended need for maintenance or renovation.

The development of the Greenlandic building industry has been a hot topic for a long time, both during the period of GTO but also since the disintegration of this organisation (which in 1987 became part of the Greenlandic home rule government under the name Nuna-tek) in 1990 [3]. An example is the report by the Directory of Buildings and Infrastructure, IAPP's, committee regarding the efficiency improvement of the building work from 2002 [4], stating that the initiatives from the prior 20–30 years were meaningful but insufficiently supported by educational and technological initiatives and active knowledge sharing. The committee concluded that the collection and dissemination of construction knowledge should be highly prioritised to improve the building processes. These issues are, however, still addressed today, 20 years later.

### *1.2. Aim and objectives*

This study presents hygrothermal measurements from nine houses in Nuuk and Sisimiut to enable evidence-based decisions on suitable construction types in Greenland. They represent three common construction types [2]: half-timber, concrete, and cross-laminated timber (CLT). The implementation of the measuring sensors, providing the data for this

* Corresponding author.
*E-mail address:* nfri@dtu.dk (N.K. Friis).

https://doi.org/10.1016/j.buildenv.2023.110686
Received 9 March 2023; Received in revised form 30 July 2023; Accepted 1 August 2023
Available online 2 August 2023

study, is independent of the construction process of the buildings. This condition allows an evaluation of the robustness of the constructions, both regarding design choices and buildability. This circumstance contrasts a previous study [5], analysing the same construction types constructed under controlled conditions and exposed to constant interior climate. The present study aims to contribute to the collected and disseminated knowledge sharing as encouraged by the AIPP committee in 2002, by answering the following research questions with a focus on the three assessed construction types:

1) Does it cause hygrothermal problems not implementing wind barriers in Greenland?

This question has become relevant, as one new construction type does not use a wind barrier. The traditional building style includes a very robust wind barrier (sealed fibre cement boards). This study focuses on the wind barriers' ability to reduce air infiltration of the insulating layers rather than increasing airtightness and eliminating thermal bridges.

2) Are all the assessed constructions robust to the Arctic climate?

In general, constructions used in the Arctic are based on building methods commonly used in milder climates; in Greenland, Danish building methods have been implemented with a few adjustments to Greenlandic conditions. However, these adjustments might not make the constructions robust for an Arctic setting.

These topics are not extensively investigated for the Arctic climate; however, there are some examples of studies evaluating the need for different membranes in cold climates. E.g., Vinha [6] investigated the hygrothermal performance of exterior timber-frame walls for multiple Finnish locations, including one above the Arctic Circle (Sodankylä). It was found that for all Finnish climates, it was safe to implement plastic vapour barriers in wall constructions. Other literature focus on other northern regions. An example is Langmans [7], who studied the feasibility of exterior air barriers in building envelopes at multiple European destinations. The study found that good workmanship and adequate material choices were essential to the airtightness of the building envelope when applying exterior air barriers. The airtightness was essential, as the purpose of the membranes was to reduce leaks in the building envelope.

Despite the existing literature regarding building quality and best practices in Arctic regions, Greenland is further challenged due to insufficient infrastructure, poor economy, and limited access to skilled labour. These limitations result in a need for a specific focus on Greenlandic conditions. However, the findings for Greenland can be applied in other Arctic regions. Therefore, this article aims to collect data from different Greenlandic building technologies and assess their performance, to benefit the construction industry in the whole Arctic region.

The remainder of this article briefly introduces specific challenges and previous projects, followed by a description of the employed methodologies and the context and setup of the monitored residential houses. Lastly, the data is analysed and discussed, leading to a conclusion.

### 1.3. Arctic building and construction

This study is a part of the research project, Arctic Building and Construction (ABC) project, which aims to identify the issues and good practices in the current construction tendencies in Greenland [8]. The ABC project primarily relies on three Greenlandic data sources. 1) a test house that experiments with sheltered unheated areas between rain screen and insulation, creating semi-indoor zones [9], 2) a test pavilion containing the most typical Greenlandic façade constructions for new constructions [5,10] and 3) hygrothermal sensors in the façades of multiple residential buildings. This study investigates the collected data from most of the monitored residential houses and compares them with results from the test pavilion [5].

As part of the ABC project, a building insulated with a new firm mineral wool insulation type was evaluated because residents complained about thermal discomfort. Theoretically, the insulation batts should eliminate the need for wind barriers when applied tightly to a concrete construction. The material had two perpendicular soft edges (flex zones) to ensure tight connections between the batts. In practice, however, the insulation was installed incorrectly and insufficiently tight, resulting in cold walls, draught, and discomfort [11]. The building was also investigated by Friis et al. [12], showing that the thermal issues could be identified by hygrothermal sensors implemented in the façade. The findings indicated that such measurements are valuable when evaluating façade performances, and similar measurements have been utilised in this study. The building façade is further presented in Section 2.1.

#### 1.3.1. The low-energy house in Sisimiut

In 2005, an experimental building was built in Sisimiut to investigate the performance of low-energy technologies in a Greenlandic context [13]. It was equipped with up to 350 mm of insulation, solar panels, a heat recovery system, and windows with low heat loss and high heat gain. In addition to the innovative installations and design decisions, the house was monitored regarding consumption of heat, hot water, and energy, the effect of the solar panel, room temperatures, and relative humidity in the construction. At the time of construction, the building regulation of 2006 [14], which is still valid in Greenland, was soon to be implemented, and the goal was to create a building which would consume only half of the permitted energy demand.

After five years, the performance was assessed, showing that it did not meet the initial ambitions [15], with an oil consumption of 140 $kWh/m^2$ compared to the calculated 80 $kWh/m^2$. According to Rode [15], the main issue was that the actual airtightness of 2.4 $l/(s{\bullet}m^2)$ was worse than the anticipated 1.5 $l/(s{\bullet}m^2)$. Still, Greenland has no demand for maximum leakage [14]. However, Rode et al. [16] estimated that poor airtightness alone might cause energy consumption to increase by 20%. The reduced airtightness indicates that the vapour barrier was insufficient, reducing the construction's robustness to the Arctic climate. Due to this and other identified issues, the building was renovated in 2018 and became part of the ABC project. Therefore, it is included in this study with its optimised building envelope, presented in Section 2.1.

#### 1.3.2. Façade membranes in the Arctic

As described in Section 1.3.1, airtightness plays a significant role in the building's heat loss and, thus, its energy consumption. In many cases, the risk of cold air infiltrating the building or insulation can be minimised by implementing wind barriers and ensuring tight material connections. Moisture can also be a severe construction problem and significantly affect the indoor climate – especially when causing rot or mould. Strategic placement of vapour barriers can influence the hygrothermal performance of a building envelope [6]. Langmans [7] found that sufficient airtightness was essential to avoid moisture issues caused by forced convection. The consequences of the presence of these membranes will be investigated in this study.

### 1.4. Moisture and mould

The moisture content ($\nu$) in the outdoor air is often very low in Greenland during winter. According to Kotol et al., it can be less than 1 $g/kg_{dry,air}$. However, cold temperatures can cause high relative humidity (RH) [17] (65%–90% RH in Nuuk 2022 [18]). The moisture excess ($\Delta\nu$) is defined as the difference between the interior and exterior moisture content. Ilomets et al. [19], conducted a field study on 237 dwelling units in cold climates and found an average moisture excess value of 2.8 $g/m^3$ during cold periods. Furthermore, $\Delta\nu$ was defined to be low when it was approximately 2 $g/m^3$ during winter. Møller and Helgason [20] evaluated the excess moisture in several buildings on Greenland's west coast and found an average of 3.9 g/m$^3$. Indoors, dry air can cause static shock and discomfort, such as eye irritation, dry skin, dermatitis causing itch, dehydration, sore throat and asthma [21].

On the other hand, high humidity levels can cause an increased risk of mould growth and elevated concentrations of house-dust mites [22]. Additionally, studies show that high relative humidity increases the risk of activating latent tuberculosis [23]. Still, tuberculosis is 20 times more common in Greenland than other Northern countries [24], with higher indoor relative humidity levels. Despite the low indoor humidity levels, mould is common in Greenlandic buildings. Some building owners try to reduce the mould growth risk by educating the residents on how to use the buildings properly [25] to ensure lower relative humidity. The strong dependency between humidity, mould growth and human health [6] makes mould growth a simple performance criterion for moisture conditions in a building.

## 2. Methods

This article is based on data collected from 4 houses in Sisimiut and 5 in Nuuk. The collected data are subjected to intercomparisons and comparison to the results of hygrothermal simulations performed in Delphin 6.1 [26]. Furthermore, the hygrothermal conditions from measurements and simulated data are analysed for mould growth risk.

### 2.1. Monitored buildings

This study includes nine buildings on the west coast of Greenland. Table 1 provides an overview of them. Four were located in Sisimiut (at the Arctic Circle), while the rest were in Nuuk, 300 km south of Sisimiut. The facades were monitored with sensors (see details in Section 2.1.2) measuring the temperature and the relative humidity at different depths in the façade. As given in Table 1, each building had different amounts of data because of the independent installation of the sensors. The monitored walls are oriented inconsistently, defined in the column "Orient". "ID" is the identification number, while "Name" is introduced to ease the understanding through this article. The houses are named depending on their construction types and the location. HT identifies half-timbered façade constructions, and CON and CLT describe concrete and cross-laminated timber constructions. "Type" presents the construction type shortly, "Year" describes the construction year, and "Angle" defines the deviance between the north façade and the north orientation. "Nr" is the number of sensors, and lastly, "Delphin years" lists for which years the individual house is assessed.

The included buildings were selected to represent the current construction tendencies. However, the primary motivation for the selection was the possibility and acceptance of implementing sensors in their facades. Additionally, drawings and descriptions of the constructions were crucial. Certain juristic precautions were necessary, including compliance with GDPR restricting the sharing of additional information about the building's locations.

#### 2.1.1. Façade constructions

The facade constructions of the nine houses presented in Table 1 are shown in Fig. 1. The number of sensors in each wall construction depends on the wind and vapour membranes implemented. In general, the sensors are placed in the air cavity, on the inner side of the wall (measuring the indoor climate) and on each side of potential vapour barriers and wind barriers. This approach results in 3–5 sensors in each wall. The sensors are coloured to match the graphs in Section 3.

House $HT_{sis3}$ is the low-energy house in Sisimiut described in Section 1.3.1, and the detail drawing shows the façade after the renovation in 2005, as the measurements are from the following period.

In the CLT-houses, $CLT_{Nuuk1}$ and $CLT_{Nuuk2}$, there are wind barriers on the exterior side of the CLT element, primarily to protect the elements from external weather conditions during construction. Kukk et al. [27] concluded that high initial moisture content in CLT panels can reduce the airtightness of CLT elements. Thus, the implemented wind barrier has two ways of contributing to the airtightness of the building, i.e., reducing the risk of cracks and reducing the airflow through leaks. The CLT is produced in Austria, but the architectural material does not define the wood species. However, it is assumed to be spruce, as this wood species is typically used in European CLT.

#### 2.1.2. Sensors

The installed HYT 221 sensors from Innovative Sensor Technology measure temperature with an accuracy of ±0.2 K within the range of 0–60 °C and RH with an accuracy of ±1.8% from 0 to 90% RH. The expected long-term drift is 0.5% RH/year and 0.05 K/year, and the operational temperature is −40 to 125 °C and 0–100% [28]. The data sheet stated that the sensors were calibrated from the factory and therefore were not calibrated as part of this study. Because of the desire to continuously measure the hygrothermal conditions in the walls, the sensors have not yet been removed and calibrated as a final endeavour of the study.

The sensors are installed with the backside towards the membranes, while the simulations provide the conditions near the surface. Optimally, the sensing part should point towards the membrane. Fig. 2 displays two examples of the sensor installation method, which is consistent for all facades. The yellow dot in the black box indicates the sensing part.

### 2.2. Hygrothermal simulations

The one-dimensional hygrothermal simulations are performed in Delphin 6.1.5 [26], which simulates coupled heat, air and moisture (HAM). Studies have validated the software and shown that the results are similar and consistent to other programs, though minor discrepancies can occur [29,30]. It is necessary to know the composition of the wall structures, the material properties, and the boundary conditions to create the models. The quality of the models was evaluated with Root Mean Square Error, RMSE. The following presents the evaluation method and the relevant details.

**Table 1**
Presentation of buildings. * Indicates that at least half of the data for the year is missing in at least one orientation. ■ Indicates the renovation year.

| | ID | Name | Type | Year | Orient | Angle | Nr | Delphin years |
|---|---|---|---|---|---|---|---|---|
| Sisimiut | 3 | $HT_{sis1}$ | Concrete w. wind barrier | 2012 | W | 7° | 5 | 2018*, 2021* |
| | 4 | $CON_{sis}$ | Concrete wo. wind barrier | 2018 | NNW, SSE | −25° | 3 | 2020, 2021, 2022 |
| | 5 | $HT_{sis2}$ | Timber frame | 2010 | NE, SE | −40° | 5 | 2021, 2022 |
| | 13 | $HT_{sis3}$ | Renovated timber frame | 2018■ | NE | 50° | 5 | 2021, 2022 |
| Nuuk | 7 | $HT_{Nuuk1}$ | Steel frame | | SE, NW | 40° | 5 | 2021, 2022 |
| | 8 | $HT_{Nuuk2}$ | Timber and steel frames | 2010 | NW | 40° | 5 | 2021 |
| | 9 | $CLT_{Nuuk1}$ | Cross-laminated timber | | NNW, SSE | −33° | 4 | 2022* |
| | 10 | $CON_{Nuuk}$ | Concrete wo. wind barrier | 2015 | SSW | 30° | 3 | 2020, 2021, 2022 |
| | 12 | $CLT_{Nuuk2}$ | Cross-laminated timber | 2016 | ESE, WNW | 30° | 4 | 2020, 2021, 2022 |

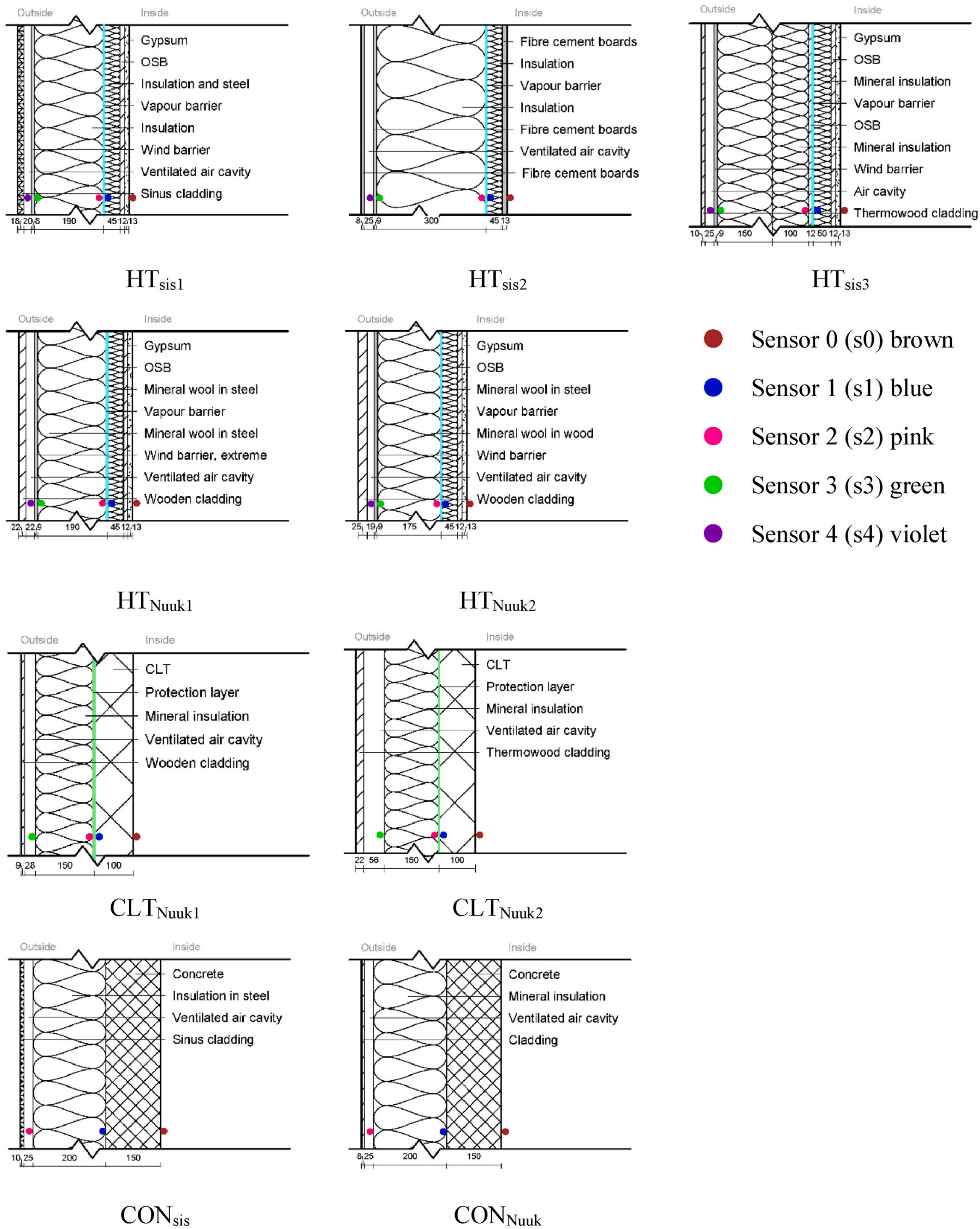


**Fig. 1.** Cross-section drawings of the wall constructions. The dots indicate the placement of sensors, and the colours refer to the graphs in Figs. 4 and 5. (For interpretation of the references to colour in this figure legend, the reader is referred to the Web version of this article.)

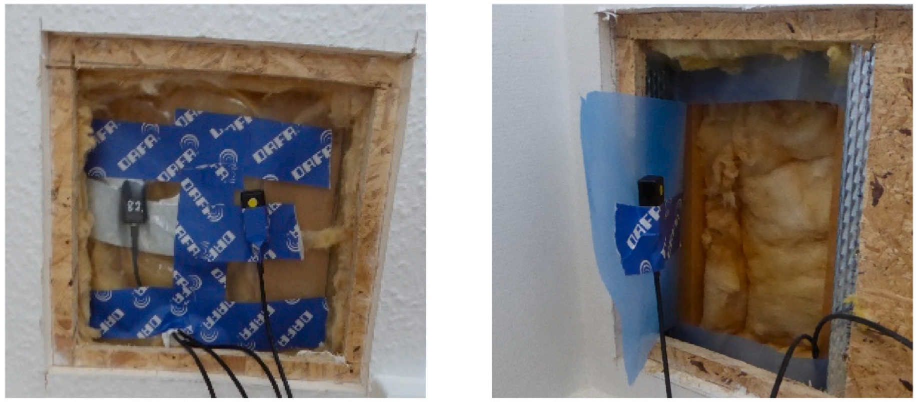

$HT_{Nuuk2}$ $HT_{sis1}$

**Fig. 2.** Example of sensor orientation near the membrane. The yellow dot is the sensing part. The membrane to the left has no colour and is transparent. (For interpretation of the references to colour in this figure legend, the reader is referred to the Web version of this article.)

### 2.2.1. Evaluation method

The accuracy of the models was identified with Root Mean Square Error, RMSE. It is calculated as presented in Eq. (1) and quantifies the error between the measured data, $x_{sensor,i}$, and simulated data, $x_{delphin,i}$. $N$ is the total amount of data points, which are individually denoted by $i$. The formula is applied on the temperature and relative humidity for each sensor. The aim is to reduce the RMSE by calibrating the models by iterations to achieve the lowest possible errors. The success criteria for RMSE are 5 °C for temperature and 10% RH.

$$\mathrm{RMSE} = \sqrt{\frac{\sum_{i=1}^{N}\left(x_{delphin,i} - x_{sensor,i}\right)^2}{N}} \quad [1]$$

Various evaluation methods have their advantages and disadvantages. The normalised RMSE (NRMSE) is often applied for its more straightforward interpretation as the unit is in percentage. However, normalised errors can magnify the errors for smaller values by removing the scale differences between the outputs [31,32]. In this study, this is a disadvantage since it involves temperature and humidity profiles through the walls, potentially leading to misinterpretation of the errors. Therefore, RMSE was chosen for this purpose. The disadvantages of using RMSE include its high sensitivity to outliers and the fact that error is always positive, neglecting whether the model is overestimating or underestimating [32,33].

### 2.2.2. Material properties

The quality of a model relies on the accuracy of the material properties. The material properties were assumed to vary as the buildings were constructed independently. The variances were defined during an iterative calibration process for each façade model. The iteration processes were based on RMSE for temperature and relative humidity.

Table 2 contains the settings for all materials for each house. Most materials were found in the Delphin database, but few were unavailable and thus defined manually. The manually defined materials were based on similar materials from the Delphin database (see respective material IDs in superscripted square brackets in Table 2) to ensure reasonable material properties regarding moisture transportation. Asterisks (*) define iterated values, while properties found in other literature and data sheets are noted with references in the specific table cell.

The exterior cladding on House $HT_{sis1}$ and $CON_{sis}$ are sinus-shaped metal sheets. The sectional drawings in Fig. 1 describe the curve sizes, while the material thickness is defined to be only 0.6 mm in the Delphin models. In the other houses, except House $HT_{sis2}$, thermowood or rough wood is applied as exterior cladding. These are problematic to define precisely due to the lack of descriptions in the available project material and the broad spectre of material properties available for these products. Thus, the material properties were adjusted by calibrating the models based on iterations.

The thermal transmittance, U-value, is calculated for each construction based on the chosen materials. Table 2 presents the essential material properties, but more detailed properties are connected to each material. These can be found in Delphin based on the material ID. The given properties, defined according to the standards in Delphin [34], include density (ρ), specific heat capacity (Cp), thermal conductivity ($\lambda$), water vapour resistance (μ), water content at saturation ($W_{sat}$), water content at 80% RH ($W_{80}$), water uptake coefficient ($A_W$), and liquid water conductivity at effective saturation ($K_{l,eff}$). All vapour barriers are defined to have a vapour diffusion thickness (sd) of 20.

### 2.2.3. Boundary conditions

The hygrothermal simulations demand hourly weather data containing temperature, relative humidity, wind direction, wind velocity, direct radiation, diffuse radiation, rain, and air pressure.

The Danish Meteorological Institute (DMI) [18] provided hourly quality-assured weather data for Nuuk. The data were free of charge but not available for Sisimiut. European Centre for Medium-Range Weather Forecasts, ECMWF, provided hourly reanalysis weather data of the relevant climate variables (ERA5) [38]. Reanalysis is a method to estimate weather conditions in a grid based on multiple surrounding weather stations. These data are also quality-assured and contain none or very few missing data. However, the data are not measured locally but are estimated for a grid structure based on available measured data.

DMI and ERA5 provide global radiation, which is then decomposed into direct and diffuse radiation using the Erbs method [39]. Missing data for solar radiation is filled in two ways. For whole days or multiple days of missing data, they are filled by interpolating the value of the same time of the day from the previous and following available day. For missing data during night-time or where the first and last hour of daylight is measured, the data are filled by interpolating the adjacent values. All other missing data are supplied by interpolation.

Fig. 3 presents selected weather parameters for all considered years. The graphs show a continuous period of missing data in 2020.

The temperature and relative humidity from the internal sensors are used to define the interior climate and are individual for each façade. Missing data are filled by linear interpolation.

For all simulations, the inner heat transmission exchange coefficient for still air was assumed to be 8 $W/m^2K$, while the vapour diffusion coefficient was set to $1e^{-8}$ s/m. On the exterior sides, the effective heat conduction exchange coefficient, including both convective and radiant heat conduction, was 25 $W/m^2K$, and the mass transfer coefficient for vapour diffusion was $5e^{-8}$ s/m. The reduction coefficients for wind-driven rain and the solar adsorption coefficient were set to 0.7, which

**Table 2**
Final material properties for each material in all houses. The U-values are given for each house in the grey headlines.

| Material | ρ | Cp | λ | μ | $W_{sat}$ | $W_{80}$ | $A_w$ | $K_{l,eff}$ |
|---|---|---|---|---|---|---|---|---|
| | Kg/m$^3$ | J/kgK | W/mK | – | Kg/m$^3$ | Kg/m$^3$ | Kg/m$^2$s$^{½}$ | s |
| House $HT_{sis1}$. U = 0.15 W/m$^2$K | | | | | | | | |
| Gypsum [81] 0.013 m | 850 | 850 | 0.200 | 10 | 551 | 7.2 | 0.28 | $6.3e^{-9}$ |
| OSB [172] 0.012 m | 630 | 1880 | 0.13 | 280 | 350 | 36.8 | 0 | $8.3e^{-11}$ |
| Insulation [730] 0.045 m | 37 | 840 | 0.032 | 1.2* | 900 | 0.1 | 0 | – |
| Vapour barrier [174] 0.0002 m | 1500 | 2100 | 0.23 | 100,000 | 0 | 0 | 0 | 0 |
| Insulation [648] 0.019 m | 168 | 840 | 0.040 | 1.7* | 900 | 0.4 | 0 | – |
| Fibre cement [265] 0.008 m | 1424 [35] | 900 [36] | 0.24 [35] | 20 [37] | 419 | 40 | 0.01 | 0 |
| Air cavity 40 mm [17] 0.20 m | 1.3 | 1050 | 0.138 | 0.4 | 1000 | 0 | 0 | 0 |
| Sinus cladding [778] 0.006 m | 7700 | 460 | 25,000 | – | – | – | – | – |
| House $HT_{sis2}$. U = 0.09 W/m$^2$K | | | | | | | | |
| Fibre cement [265] 0.13 m, 0.09 m, 0.08 m | 1424 [35,35] | 900 [36] | 0.24 [35] | 20 [37] | 419 | 40 | 0.01 | 0 |
| Insulation [731] 0.045 m | 67 | 840 | 0.035 | 1 | 900 | 0.1 | 0 | – |
| Vapour barrier [174] 0.0002 m | 1500 | 2100 | 0.23 | 100,000 | 0 | 0 | 0 | 0 |
| Insulation [731] 0.03 m | 67 | 840 | 0.035 | 1 | 900 | 0.1 | 0 | – |
| Air cavity 25 mm [16] 0.25 m | 1.3 | 1050 | 0.138 | 0.4 | 1000 | 0 | 0 | 0 |
| House $HT_{sis3}$. U = 0.12 W/m$^2$K | | | | | | | | |
| Gypsum [81] 0.013 m | 850 | 850 | 0.200 | 10 | 551 | 7.2 | 0.28 | $6.3e^{-9}$ |
| OSB [172] 0.012 m, 0.012 m | 630 | 1880 | 0.130 | 280 | 350 | 36.8 | 0 | $8.3e^{-11}$ |
| Insulation [730] 0.050 m | 37 | 840 | 0.032 | 1 | 900 | 0.1 | 0 | – |
| Vapour barrier [174] 0.0002 m | 1500 | 2100 | 0.230 | 100,000 | 0 | 0 | 0 | 0 |
| Insulation [648] 0.1 m, 0.15 m | 168 | 840 | 0.040 | 1 | 900 | 0.4 | 0 | – |
| Fibre cement [265] 0.009 m | 1424 [35] | 900 [36] | 0.24 [35] | 20 [37] | 419 | 40 | 0.01 | 0 |
| Air cavity 25 mm [16] 0.025 m | 1.3 | 1050 | 0.138 | 0.4 | 1000 | 0 | 0 | 0 |
| Thermowood [654] 0.008 m | 1158.7 | 1188 | 0.313 | 26.40 | 283.6 | 70.9 | 0.01 | $2.5e^{-12}$ |
| House $HT_{Nuuk1}$. U = 0.15 W/m$^2$K | | | | | | | | |
| Gypsum [81] 0.013 m | 850 | 850 | 0.200 | 10 | 551 | 7.2 | 0.28 | $6.3e^{-9}$ |
| OSB [172] 0.012 m | 630 | 1880 | 0.13 | 280 | 350 | 36.8 | 0 | $8.3e^{-11}$ |
| Insulation [730] 0.045 m | 37 | 840 | 0.032 | 1 | 900 | 0.1 | 0 | – |
| Vapour barrier [174] 0.0002 m | 1500 | 2100 | 0.23 | 100,000 | 0 | 0 | 0 | 0 |
| Insulation [648] 0.190 m | 168 | 840 | 0.040 | 1 | 900 | 0.4 | 0 | – |
| Fibre cement [265] 0.009 m | 1424 [35] | 900 [36] | 0.24 [35] | 20 [37] | 419 | 40 | 0.01 | 0 |
| Air cavity 25 mm [16] 0.022 m | 1.3 | 1050 | 0.138 | 0.4 | 1000 | 0 | 0 | 0 |
| Cladding [654] 0.022 m | 1158.7 | 1188 | 0.313 | 26.4 | 283.6 | 70.9 | 0.01 | $2.5e^{-12}$ |
| House $HT_{Nuuk2}$. U = 0.15 W/m$^2$K | | | | | | | | |
| Gypsum [81] 0.013 m | 850 | 850 | 0.16* | 10 | 551 | 7.2 | 0.28 | $6.3e^{-9}$ |
| OSB [172] 0.012 m | 630 | 1880 | 0.13 | 280 | 350 | 36.8 | 0 | $8.3e^{-11}$ |
| Insulation [730] 0.045 m | 37 | 840 | 0.032 | 1 | 900 | 0.1 | 0 | – |
| Vapour barrier [174] 0.0002 m | 1500 | 2100 | 0.23 | 100,000 | 0 | 0 | 0 | 0 |
| Insulation [648] 0.175 m | 168 | 840 | 0.04* | 1 | 900 | 0.4 | 0 | – |
| Fibre cement [265] 0.009 m | 1424 [35] | 900 [36] | 0.24 [35] | 20 [37] | 419 | 40 | 0.01 | 0 |
| Air cavity 40 mm [17] 0.019 m | 1.3 | 1050 | 0.138 | 0.4 | 1000 | 0 | 0 | 0 |
| Cladding [654] 0.025 m | 1158.7 | 1188 | 0.313 | 26.4 | 283.6 | 70.9 | 0.01 | $2.5e^{-12}$ |
| House $CLT_{Nuuk1}$. U = 0.19 W/m$^2$K | | | | | | | | |
| CLT [626] 0.100 m | 425 | 1245 | 0.120 | 73 | 590.2 | 72.6 | 0 | $9.5e^{-10}$ |
| Wind barrier [28] 0.0001 m | 1200 | 2000 | 0.145 | 15,000 | 2.5 | 0 | 0 | – |
| Insulation [731] 0.150 m | 67 | 840 | 0.035 | 1 | 900 | 0.1 | 0 | – |
| Air cavity 40 mm [17] 0.028 m | 1.3 | 1050 | 0.138 | 0.4 | 1000 | 0 | 0 | 0 |
| Wood cladding [279] 0.009 m | 1250 | 1100 | 0.580 | 80 | 260 | 59.5 | 0 | – |
| House $CLT_{Nuuk2}$. U = 0.19 W/m$^2$K | | | | | | | | |
| CLT [626] 0.100 m | 425 | 1245 | 0.120 | 73 | 590.2 | 72.6 | 0 | $9.5e^{-10}$ |
| Wind barrier [28] 0.0001 m | 1200 | 2000 | 0.145 | 15,000 | 2.5 | 0 | 0 | – |
| Insulation [731] 0.150 m | 67 | 840 | 0.035 | 1.7* | 900 | 0.1 | 0 | – |
| Air cavity 56 mm [16] 0.560 m | 1.3 | 1050 | 0.138 | 0.4 | 1000 | 0 | 0 | 0 |
| Cladding [654] 0.022 m | 600* | 1188 | 0.2* | 26.4 | 283.6 | 70.9 | 0.01 | $2.5e^{-12}$ |
| House $CON_{sis}$. U = 0.17 W/m$^2$K | | | | | | | | |
| Concrete [569] 0.150 m | 2104.2 | 1000 | 2.100 | 76.12 | 219.9 | 102.3 | 0.1 | $2.7e^{-10}$ |
| Insulation [731] 0.200 m | 67 | 840 | 0.035 | 1 | 900 | 0.1 | 0 | – |
| Air cavity 25 mm [16] 0.025 m | 1.3 | 1050 | 0.138 | 0.4 | 1000 | 0 | 0 | 0 |
| Sinus cladding [778] 0.0006 m | 7700 | 460 | 25,000 | – | – | – | – | – |
| House $CON_{Nuuk}$. U = 0.17 W/m$^2$K | | | | | | | | |
| Concrete [569] 0.150 m | 2104.2 | 1000 | 2.100 | 76.12 | 219.9 | 102.3 | 0.1 | $2.7e^{-10}$ |
| Insulation [731] 0.200 m | 67 | 840 | 0.035 | 1.7* | 900 | 0.1 | 0 | – |
| Air cavity 25 mm [16] 0.025 m | 1.3 | 1050 | 0.138 | 0.4 | 1000 | 0 | 0 | 0 |
| Cladding [654] 0.0008 m | 1158.7 | 1188 | 0.313 | 26.4 | 283.6 | 70.9 | 0.01 | $2.5e^{-12}$ |

is standard for vertical walls in Delphin. Additionally, the grids for simulation are defined based on the standards for Delphin, i.e., minimum 1 mm and maximum 50 mm, with a stretch factor of 1.3. The initial hygrothermal conditions are defined as 20 °C and 50% RH.

*2.2.4. Ventilated air cavities*

All considered wall constructions have a ventilated air cavity. The air change rate (ACH) in the cavity is problematic to quantify, both theoretically and experimentally. In a similar study, the quality of the Delphin models was found insensitive to this factor [5]; however, it does affect the RMSE in the external layers of the construction. Because of the complexity in quantifying the ACH [40–42] and the varying conditions in this study, the value was iterated within the range from 0 to 650 $h^{-1}$ [43]. The initial setpoint is 60 $h^{-1}$.

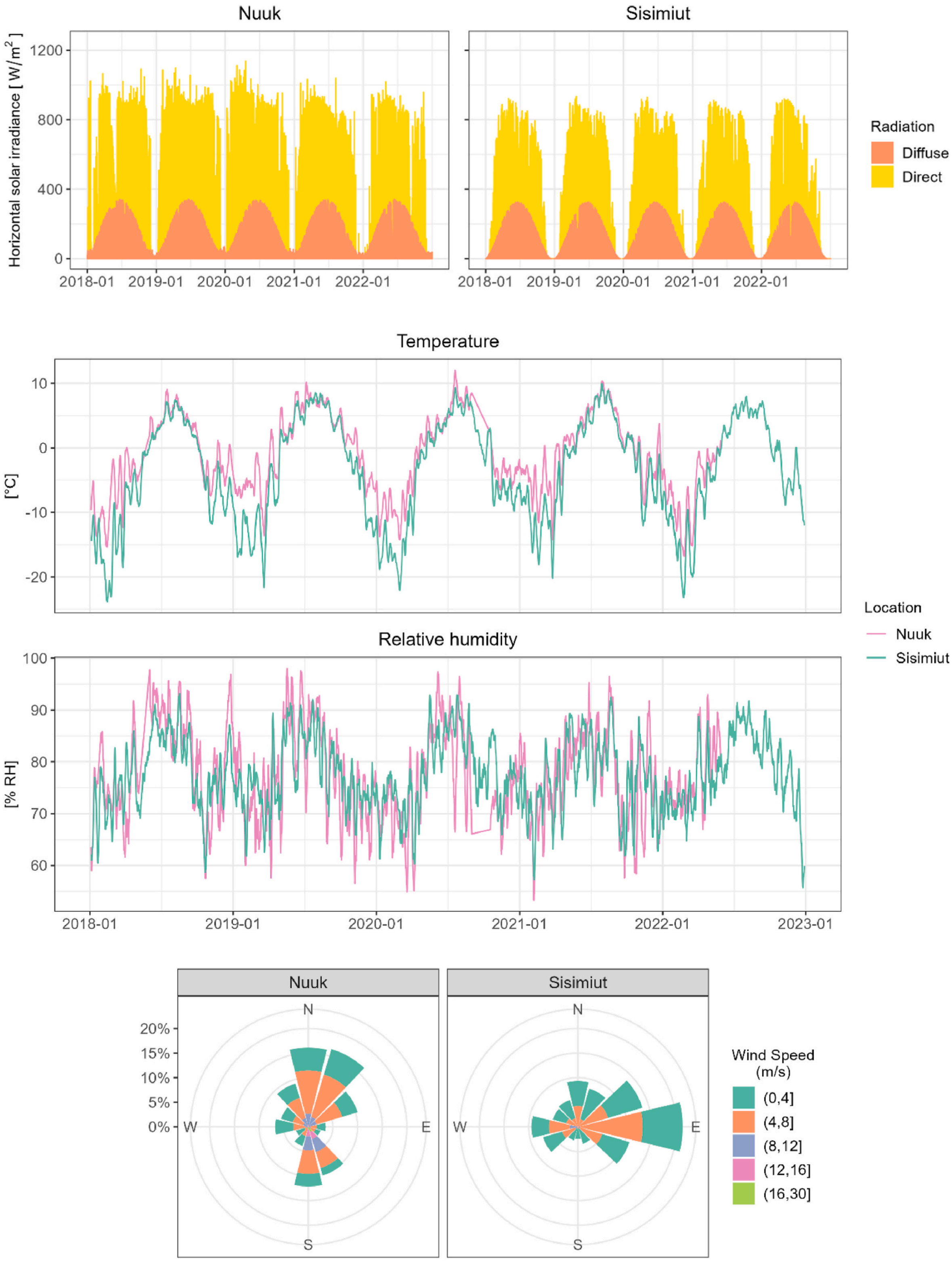


**Fig. 3.** Weather data for Nuuk (DMI) and Sisimiut (ERA5) for the time of sensor data from the nine houses.

### *2.3. Mould index and evaluation of membranes*

According to SBI 277, the risk of mould growth depends on the amount of moisture, the temperature, the availability of nutrition and time. The growth risk is high for temperatures between 20 and 30 °C, and the critical level for wood is 75% RH and higher for other materials [44].

Based on the measured conditions for each sensor point, the mould growth risk was determined for all evaluated facades by using the Viitanen model [45], which is the underlying method in the software “WUFI Mould INDEX VTT 2.3” [46]. Additionally, three houses (one of each construction type) in Nuuk were picked to investigate the consequences of present and absent membranes. Four scenarios were set up and analysed:

1. Applied wind barrier but no vapour barrier.
2. Applied vapour barrier but no wind barrier.
3. No membranes.
4. Both membranes.

In the Viitanen model, the nutrition level for potential mould is defined as the sensitivity of a material. The available sensitivity classes are “very sensitive”, “sensitive”, “medium-resistant”, or “resistant” [47]. The “very sensitive” predefined pine sapwood material was selected for the general assessments. This property reflects the worst-case scenarios, as some exposed materials are less sensitive. An additional assessment has been made to match the actual conditions for these layers.

The mould growth rates are indexed from 0 to 6, where 0 equals no growth. Indexes 1 and 2 are used for small amounts or several local colonies on a microscopic level, while indexes 3 and above are used for visually present or large amounts of microscopic mould [47]. The mould growth index inside constructions is acceptable if it is below 2. As mould growth is one of the first indications of biological deterioration, it is an excellent hygrothermal performance criterion [48].

## 3. Results and analysis

This section presents the most important results and visualisations from the assessments performed according to Section 2. Additional graphs and data can be found in the repository [49].

### 3.1. Visual assessment of measured data

The graphs in Fig. 4 present the measured data for each house as a moving mean of 7 days. The graphs are provided to give an overview of the quantity of collected data points, which varies for each building, and in some cases, for each orientation due to technical circumstances. Each orientation’s interior climate is unique as the sensors are placed in different rooms. Larger versions of the graphs are presented in the repository [49].

Unfortunately, the amount of data for $HT_{sis1}$ is minimal due to technical issues disrupting the constant logging. Despite the missing data, it was included to represent the west-oriented half-timber facades in Sisimiut. The graphs for $HT_{sis1}$ show that the temperatures are almost identical on both sides of the wind barrier (s3 and s4), while the relative humidity decreases considerably on the inner side of this construction element.

For $HT_{sis2}$, there are more available data points for the SE than NE orientation. In the SE orientation, the relative humidity in the external layers is generally higher in SE than in NE. On the other hand, the temperatures are higher in the internal layers in NE to SE. However, the interior climates are very similar for both orientations.

The fact that the temperature in s2 is higher than in s1 in $HT_{sis2[SE]}$ indicates that at least one of the sensors has drifted or that the error of the sensors exceeds the temperature difference at the two measurement points. There is no obvious explanation for the warmer temperatures on the exterior of the thin vapour barrier, which has a relatively high thermal conductivity, λ.

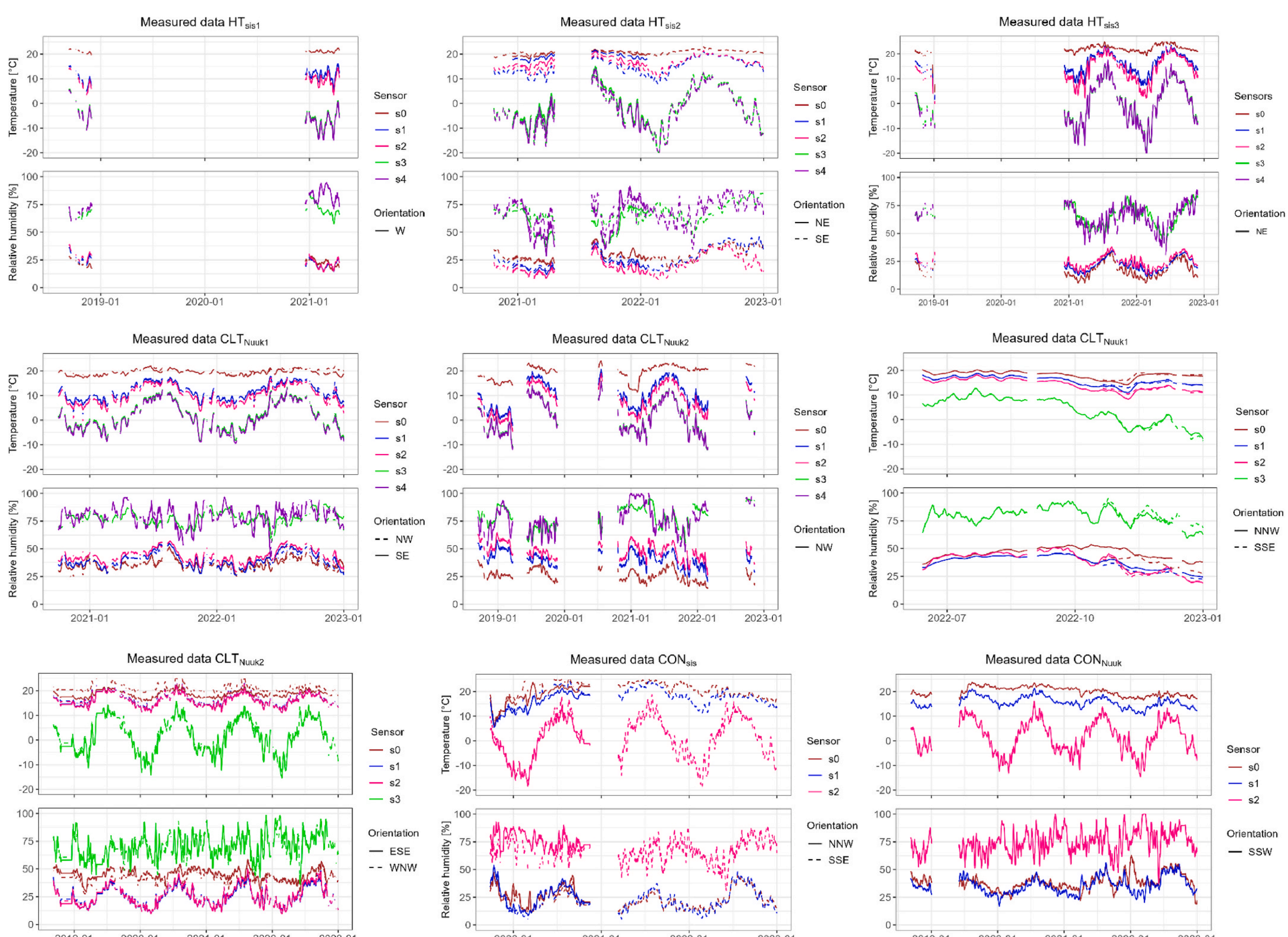

**Fig. 4.** Presentation of all measured data for each building, including temperature and relative humidity. All graphs are displayed for moving mean values of 7 days.

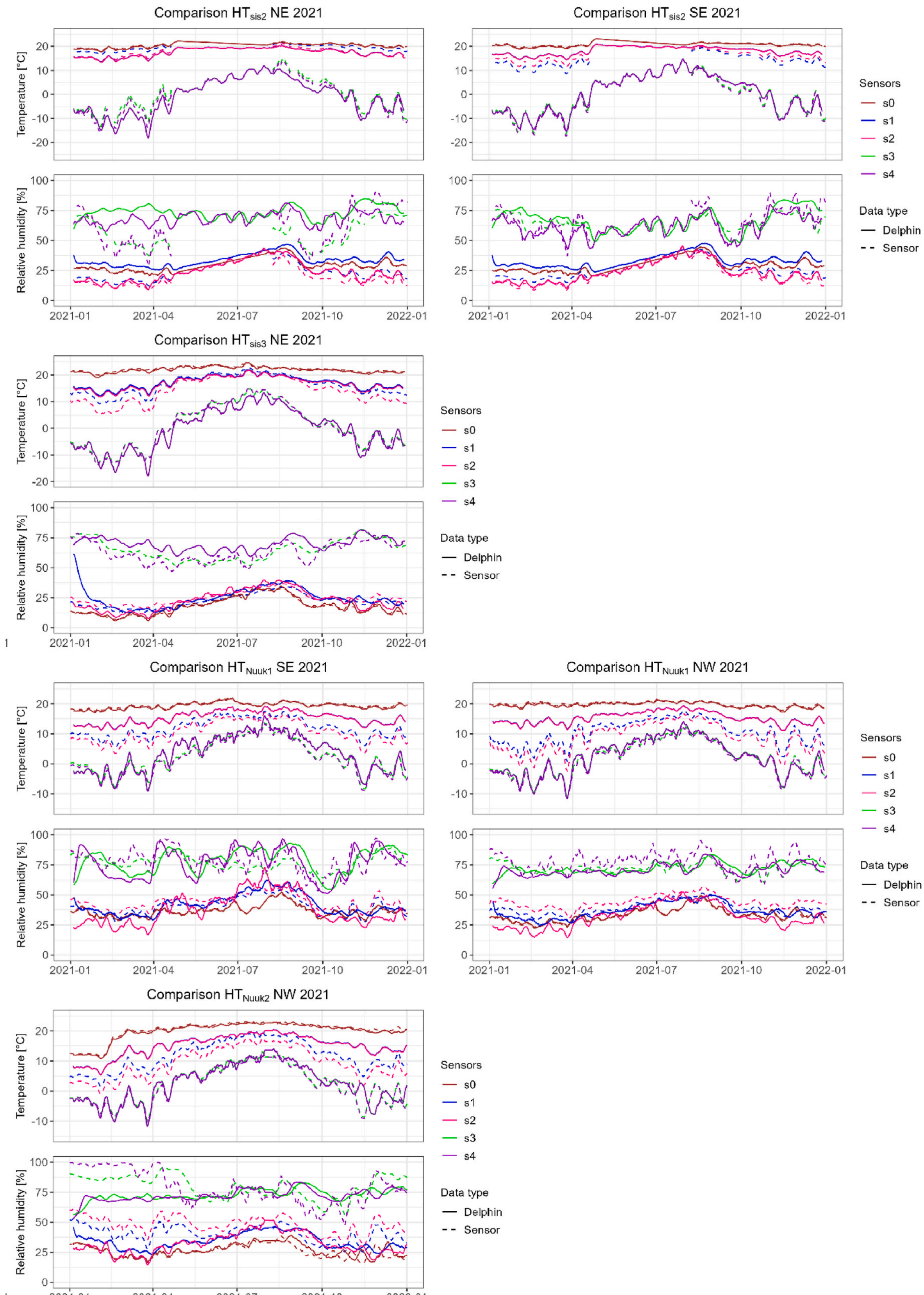


**Fig. 5.** Comparison of the measured hygrothermal conditions and the results of Delphin models for selected houses, orientations, and years. All graphs are displayed for moving mean values of 7 days.

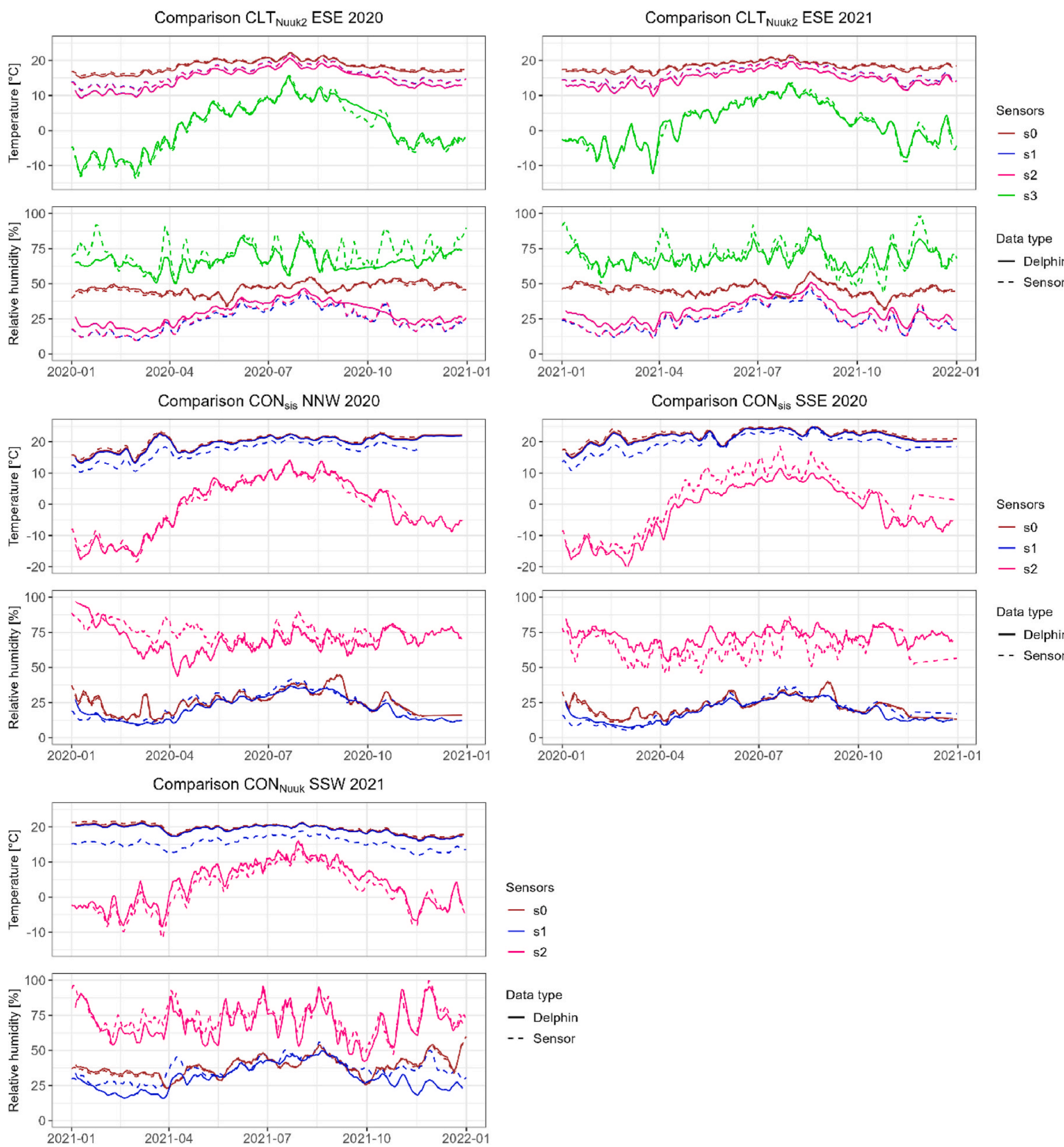


**Fig. 5.** (*continued*).

The conditions in $HT_{Nuuk1}$ are very similar for both orientations, making it difficult to see the lines for NW in the graphs. The interior temperatures in $HT_{Nuuk2}$ vary more than in the other buildings. At one point in spring 2021, the room temperature drops while the relative humidity increases to 100%.

In $CLT_{Nuuk2}$, the interior conditions are very different in ESE and WNW, but it does impact the conditions in the wall construction.

For the short periods in $CON_{sis}$, where multiple orientations are logged, the temperature and RH are similar for both orientations. The interior temperatures are, however, a bit low at the beginning and end of the measured period. In the graph for $CON_{Nuuk}$, the temperature difference between s0 and s1 is larger than in $CON_{sis}$.

Based on the graphs in Fig. 4 presenting all measured data, specific years for each house are chosen for simulations. Representative years are chosen, considering those with fewer missing data. For houses with multiple orientations, years with available data from both orientations are selected.

### 3.2. *Comparison of measured and simulated data*

#### 3.2.1. *Visual comparison*

The graphs in Fig. 5 show the moving means of 7 days of the measured data compared to the simulated data produced in Delphin. The figure contains graphs for selected years and orientations, but all produced graphs can be found in the repository [49]. A general observation is that the temperature gap between s1 and s2 in constructions with vapour barriers (all five half-timber constructions) is more significant for the measured data than the simulated data. The reason for this can be traced back to the orientation of the sensing part of the sensors, which, on both sides, are installed with the backside towards the membrane, see Fig. 2. This method creates a longer distance and, thus, an increased temperature difference between the two sensors.

In $HT_{Nuuk1 [NW]}$, however, the difference is more significant all year, which is also presented later by the RMSE in Table 3. All other half-timber constructions are graphically evaluated for 2021. For $HT_{sis3 [NE]}$, $HT_{Nuuk1 [SE]}$, and $HT_{Nuuk1 [NW]}$, the tendencies are the same for 2021

**Table 3**
RMSE of all simulated models. Yellow cells exceed the defined success criteria. Grey cells indicate sensors, which are suspected of drifting.

| | Year | RMSE of Temperature [°C] | | | | | RMSE of RH [% RH] | | | | | RMSE of RH (mm of 7 days) [% RH] | | | | | NA's | ACH [$h^{-1}$] |
|---|---|---|---|---|---|---|---|---|---|---|---|---|---|---|---|---|---|---|
| | | S0 | S1 | S2 | S3 | S4 | S0 | S1 | S2 | S3 | S4 | S0 | S1 | S2 | S3 | S4 | | |
| Sisimiut (ERA5 weather data) | | | | | | | | | | | | | | | | | | |
| $HT_{sis1[W]}$ | 2018 | 0.5 | 4.4 | 5.7 | 8.7 | 8.8 | 1.0 | 8.5 | 10.6 | 5.6 | 9.8 | 0.8 | 5.7 | 9.8 | 5.1 | 8.0 | 7877 | 60 |
| $HT_{sis1[W]}$ | 2021 | 0.5 | 4.7 | 6.2 | 8.2 | 8.5 | 0.9 | 9.7 | 8.9 | 6.5 | 13.3 | 0.5 | 7.5 | 8.1 | 5.7 | 11.9 | 6252 | 60 |
| $HT_{sis2[NE]}$ | 2021 | 0.3 | 2.5 | 1.0 | 5.5 | 5.4 | 1.1 | 13.0 | 9.1 | 22.3 | 20.1 | 0.4 | 11.6 | 4.4 | 22.2 | 16.0 | 2479 | 90 |
| $HT_{sis2[SE]}$ | 2021 | 0.3 | 3.6 | 2.1 | 3.2 | 3.6 | 1.1 | 11.5 | 9.3 | 8.7 | 13.1 | 0.4 | 9.6 | 2.1 | 6.9 | 6.2 | 2479 | 120 |
| $HT_{sis2[SE]}$ | 2022 | 0.3 | 2.5 | 1.4 | 2.8 | 3.1 | 1.1 | 9.5 | 8.0 | 7.2 | 14.3 | 0.4 | 7.9 | 1.6 | 5.9 | 8.4 | 3 | 120 |
| $HT_{sis3[NE]}$ | 2021 | 0.5 | 2.3 | 4.3 | 3.1 | 3.6 | 0.7 | 8.4 | 5.7 | 8.1 | 16.3 | 1.2 | 6.0 | 4.4 | 7.1 | 9.8 | 3 | 60 |
| $HT_{sis3[NE]}$ | 2022 | 0.5 | 2.4 | 4.3 | 3.4 | 3.8 | 0.7 | 7.7 | 6.1 | 9.0 | 16.3 | 1.1 | 5.6 | 4.9 | 8.3 | 9.9 | 748 | 60 |
| $CON_{sis[NNW]}$ | 2020 | 0.7 | 2.6 | 4.9 | – | – | 1.6 | 4.8 | 17.5 | – | – | 0.9 | 3.8 | 10.2 | – | – | 1836 | 60 |
| $CON_{sis[SSE]}$ | 2020 | 0.7 | 2.4 | 7.1 | – | – | 1.3 | 4.3 | 19.2 | – | – | 0.9 | 3.3 | 10.8 | – | – | 2379 | 160 |
| $CON_{sis[SSE]}$ | 2021 | 0.7 | 2.4 | 7.2 | – | – | 1.2 | 4.0 | 18.4 | – | – | 0.8 | 2.9 | 9.2 | – | – | 1732 | 160 |
| $CON_{sis[SSE]}$ | 2022 | 0.7 | 2.9 | 6.2 | – | – | 1.3 | 4.5 | 18.4 | – | – | 0.8 | 2.8 | 10.8 | – | – | 84 | 160 |
| Nuuk (DMI weather data) | | | | | | | | | | | | | | | | | | |
| $HT_{Nuuk1[SE]}$ | 2021 | 0.7 | 4.0 | 5.4 | 5.3 | 5.5 | 4.9 | 8.4 | 14.5 | 10.6 | 17.0 | 0.8 | 4.6 | 10.6 | 9.3 | 10.5 | 44 | 30 |
| $HT_{Nuuk1[NW]}$ | 2021 | 1.3 | 5.8 | 7.6 | 3.3 | 3.5 | 4.5 | 7.1 | 15.1 | 7.1 | 14.3 | 0.8 | 3.3 | 13.6 | 5.6 | 9.2 | 286 | 30 |
| $HT_{Nuuk1[SE]}$ | 2022 | 0.4 | 3.1 | 4.3 | 3.4 | 3.3 | 1.5 | 8.1 | 13.1 | 9.9 | 14.7 | 0.8 | 3.7 | 10.8 | 9.2 | 9.1 | 11 | 30 |
| $HT_{Nuuk1[NW]}$ | 2022 | 0.5 | 5.1 | 6.9 | 1.4 | 1.4 | 1.6 | 6.9 | 14.3 | 5.9 | 13.1 | 0.7 | 2.1 | 12.5 | 5.1 | 9.4 | 130 | 30 |
| $HT_{Nuuk2[NW]}$ | 2021 | 0.9 | 4.4 | 6.6 | 4.6 | 4.7 | 5.6 | 12.0 | 20.0 | 14.5 | 20.4 | 3.8 | 9.6 | 18.6 | 13.6 | 17.8 | 291 | 15 |
| $CLT_{Nuuk1[NNW]}$ | 2022 | 0.4 | 1.0 | 0.9 | 2.0 | – | 1.1 | 2.9 | 2.8 | 9.8 | – | 0.9 | 2.6 | 2.2 | 3.6 | – | 3842 | 160 |
| $CLT_{Nuuk1[SSE]}$ | 2022 | 0.4 | 1.0 | 1.0 | 2.9 | – | 1.1 | 2.6 | 2.8 | 12.0 | – | 0.9 | 2.1 | 2.2 | 6.7 | – | 4512 | 400 |
| $CLT_{Nuuk2[ESE]}$ | 2020 | 0.4 | 1.0 | 0.9 | 2.0 | – | 1.1 | 2.9 | 2.8 | 9.8 | – | 0.9 | 2.6 | 2.2 | 3.6 | – | 12 | 90 |
| $CLT_{Nuuk2[WNW]}$ | 2020 | 0.4 | 1.0 | 1.0 | 2.9 | – | 1.1 | 2.6 | 2.8 | 12.0 | – | 0.9 | 2.1 | 2.2 | 6.7 | – | 65 | 180 |
| $CLT_{Nuuk2[ESE]}$ | 2021 | 0.4 | 1.4 | 1.4 | 3.6 | – | 1.9 | 6.3 | 6.1 | 14.4 | – | 1.2 | 5.2 | 4.6 | 8.3 | – | 49 | 90 |
| $CLT_{Nuuk2[WNW]}$ | 2021 | 0.5 | 0.9 | 0.7 | 2.9 | – | 1.6 | 4.2 | 4.2 | 12.7 | – | 1.2 | 2.9 | 2.8 | 6.7 | – | 96 | 180 |
| $CLT_{Nuuk2[ESE]}$ | 2022 | 0.4 | 1.3 | 1.3 | 3.1 | – | 1.9 | 6.6 | 6.4 | 12.3 | – | 1.1 | 6.0 | 5.3 | 6.4 | – | 24 | 90 |
| $CLT_{Nuuk2[WNW]}$ | 2022 | 0.5 | 0.9 | 0.7 | 2.4 | – | 1.6 | 4.1 | 4.0 | 10.4 | – | 1.2 | 3.1 | 3.0 | 5.3 | – | 86 | 180 |
| $CON_{Nuuk[SSW]}$ | 2020 | 0.5 | 1.1 | 1.1 | 3.0 | – | 1.9 | 5.2 | 5.1 | – | – | 1.2 | 4.6 | 3.9 | – | – | 18 | 30 |
| $CON_{Nuuk[SSW]}$ | 2021 | 0.6 | 1.0 | 0.7 | 2.3 | – | 1.6 | 3.7 | 3.5 | – | – | 1.2 | 2.3 | 2.1 | – | – | 254 | 30 |
| $CON_{Nuuk[SSW]}$ | 2022 | 0.5 | 4.5 | 5.4 | 5.9 | – | 1.9 | 9.3 | 18.2 | – | – | 1.0 | 8.5 | 12.3 | – | – | 485 | 30 |

and 2022. Delphin simulates a higher RH than measured at s3 and s4 in $HT_{sis3[NE]}$ and $HT_{Nuuk1[SE]}$. For all three facades, the measured temperatures in s1 and s2 are lower during winter than in the simulations. $HT_{sis1}$ is not visualised due to the high number of missing data (see Fig. 4). For $HT_{sis2}$, the Delphin model resembles the wall facing SE more closely than NE, as the measured RH in the air cavity in the latter is much lower than the simulated values.

The graphs for $CLT_{Nuuk2}$ are only presented for the 2020 and 2021 ESE orientation, as the tendencies are the same for WNW during all three assessed years. The graphs for 2020 are more inaccurate and have a bigger RMSE, which is presented in Table 3. The graphs for $CLT_{Nuuk1}$ are excluded due to the well-fitted models, indicating that the wall performs as expected. The excluded graphs can be found in the repository [49].

$CON_{Nuuk}$ is represented for the year 2021, where the humidity level in s1 is lower in the measured data than in the simulation. $CON_{sis}$ is represented for 2020, showing that the simulation of RH is generally a bit low for NNW and a bit high for SSE, which might be a consequence of the temperature simulation being lower than the measured data in SSE. Generally, the model fits better to the measurements from $CON_{sis}$ than from $CON_{Nuuk}$, despite the very similar constructions and thus similar models.

### 3.2.2. Root mean square errors

As explained in Section 2.2.1, RMSE is used to determine the accuracy of the simulations. Eq. (1) calculates the RMSE, and the results are presented in Table 3. The yellow cells indicate the errors, exceeding the defined success criteria of 5 °C for temperature and 10% for RH. Regardless of the weather data source and location, a general observation is that the layers close to the exterior climate perform worse than the interior layers. Additionally, the models are better fitted to temperature than to RH. This difference might partly be because the temperature development through the façade is adjusted by the thermal conductivity, λ, alone, while multiple parameters define the moisture conditions. The relative humidity also depends on the temperature, as hot air can contain more moisture than cold air. The last two columns in Table 3 describe the number of missing data (NAs) and the final air change rate (ACH) in the ventilated air cavity in the model. As the RMSE evaluation method is sensitive to outliers [33], the error for RH is also given for the 7-day moving mean to indicate how well the model follows the measured trends. The south-facing walls in Sisimiut generally have a higher ACH than the remaining orientations at this location, but there is no similar tendency for Nuuk.

The RMSEs for moving means of relative humidity are generally much lower than for the original measured and simulated data, especially in the exterior layers, close to the climate conditions, which vary more than the relatively stable interior climates.

The previous study, presented in Section 1.3 [12], found that $CON_{Nuuk}$ did not perform acceptably, as the temperatures at s1 were very low. However, the RMSE at s1 was within the defined limitations. This discrepancy emphasises the value of including multiple indicators, e.g., statistical errors and visualisations, to identify potential issues. When comparing the error for $CON_{Nuuk}$ at s1 with the remaining constructions, other measured data might also be critical or deviate from the simulated data. Especially the half-timber constructions including $HT_{Nuuk1[SE]}$, $HT_{Nuuk1[NW]}$, $HT_{Nuuk2[NW]}$, and $HT_{sis1[W]}$ show deviations. This observation is stressed by the graphic visualisations in Fig. 5. The RMSEs for relative humidity in $HT_{Nuuk2[NW]}$ and $HT_{sis2[NE]}$ are very high. For $HT_{sis2}$, the errors for the NE are larger than for the SE orientation, both regarding RMSE and visually. In $HT_{Nuuk2[NW]}$, the errors are also large for the temperatures, which might affect the relative humidity results.

### 3.3. Mould indexes and membranes

The mould growth indexes are calculated to identify the robustness of the constructions for the Arctic climate. Of the nine houses, $HT_{sis1}$, $HT_{sis2}$, $HT_{Nuuk1}$, $CLT_{Nuuk1}$, and $HT_{sis3}$ are equipped with both a vapour barrier and wind barrier, while $HT_{Nuuk2}$ and $CLT_{Nuuk2}$ are equipped with only a wind barrier, and $CON_{sis}$ and $CON_{Nuuk}$ have no membranes at all.

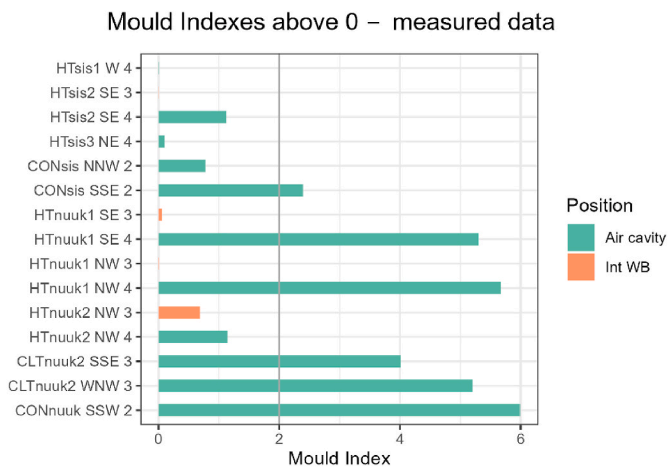


**Fig. 6.** Mould indexes above 0 for all measured data from the first to the last data point, with material class "very sensitive".

Despite the "very sensitive" applied sensitivity level, most mould indexes simulated with WUFI were 0, equal to no risk. Fig. 6 presents all the sensor points where the mould index was above 0. The blue vertical line indicates the threshold of 2 for an acceptable mould index. Common for all critical indexes is that the sensor point is either inside the air cavity or on the internal side of the wind barrier. According to Wang et al. [50], the risk of mould growth in a ventilated air cavity is reduced because of the constant airflow. The number of available data can impact the results, and Fig. 4 and Table 3 show the missing data for each house. One year consists of 8760 measurements, except the leap year 2020, consisting of 8784 measurements. The missing data were interpolated to create a continuous series of measurements for at least one year, which is necessary to simulate with the WUFI software.

In $HT_{Nuuk1}$, the mould indexes are zero at all sensor positions in the NE-facing façade, while there is a higher risk in the SE-facing façade, both in the air cavity and on the interior side of the wind barrier. None of the indexes in $HT_{Nuuk1}$ exceeds the critical level of 2. In $CON_{Nuuk[SSW]}$, only the air cavity was at risk for mould growth; however, it was severely high.

Based on the results from Fig. 6, the number of missing data, and the interest in testing each construction type, $HT_{Nuuk1[SE]}$ (2022), $CON_{Nuuk[SSW]}$ (2021), and $CLT_{Nuuk2[ESE]}$ (2021) were chosen for the four test scenarios presented in Section 2.3. The original structure of $HT_{Nuuk1}$, including both membranes, is equal to Test 4, while the initial construction for $CON_{Nuuk}$, excluding both membranes, is equal to Test 3. The initial construction for $CLT_{Nuuk2}$ is equal to Test 1, as it includes only the wind barrier. All initial test formats are visualised with grey cells in Table 4. For both $CON_{Nuuk[SSW]}$ and $CLT_{Nuuk2}$, extra membranes are implemented. New sensor names are introduced in Table 4 to keep the original connection between sensor numbers and positions. For $CON_{Nuuk[SSW]}$, "1x" describes the new sensor point on the exterior side of the implemented vapour barrier, and "2i" is the sensor point on the inner side of the implemented wind barrier. "1i" describes the interior side of the implemented vapour barrier in $CLT_{Nuuk2}$. The red values indicate mould indexes above 2, and the values in brackets are the indexes for the measured data. All mould indexes are calculated for a period equal to the measured period. As described in Section 2.3, the mould indexes are generally calculated for the "very sensitive" material class to identify the worst-case scenarios. For the assessments of the barriers, the indexes were also calculated for medium-resistant sensitivity in layers where the materials were fit for this definition (excluding points with no risk at higher sensitivity classes). The results for medium-resistant sensitivity are presented superscripted after an asterisk (*) in Table 4. In the air cavity of $HT_{Nuuk1}$, the battens keeping the cladding in place are made of raw wood. Therefore, the sensitivity is not reduced in this layer.

**Table 4**
Mould indexes for test scenarios in the constructions of $HT_{Nuuk1[SE]}$, $CON_{Nuuk[SSW]}$, and $CLT_{Nuuk2[ESE]}$. Brackets contain the index for measured data. Red numbers exceed the accepted index of 2. The durations vary according to the number of measured data to make the indexes comparable. Asterisks (*) followed by numbers are results for the medium-resistant sensitivity class due to the absence of wood. $HT_{Nuuk1[SE]}$ is a steel construction.

| | | | | | | |
|---|---|---|---|---|---|---|
| Wind barrier | | | + | – | – | + |
| Vapour barrier | | | – | + | – | + |
| | Position | | Test 1 | Test 2 | Test 3 | Test 4 |
| $HT_{Nuuk1}$ [SE] | Int VB | 1 | 0.0 | 0.0 | 0.0 | 0.0 (0.0) |
| | Ext VB | 2 | – | 0.0 | – | 0.0 (0.0) |
| | Int WB | 3 | $3.8^{*0.04}$ | – | – | $3.7^{*0.04}$ (0.1) |
| | Air cavity | 4 | 5.4 | 5.4 | 5.4 | 5.4 (5.3) |
| $CON_{Nuuk}$ [SSW] | Int VB | 1 | 0.0 | 0.05 | 0.0 (0.0) | 0.0 |
| | Ext VB | 1x | – | 0.0 | – | 0.0 |
| | Int WB | 2i | $0.04^{*0.0}$ | – | – | $0.1^{*0.0}$ |
| | Air cavity | 2 | $5.3^{*0.018}$ | $5.4^{*0.021}$ | 5.4 (6.0) $^{*0.02}$ | $5.3^{*0.018}$ |
| | Outside | 3 | $6.0^{*0.026}$ | $6.0^{*0.029}$ | 6.0 (6.0) $^{*0.029}$ | $6.0^{*0.027}$ |
| $CLT_{Nuuk2}$ [ESE] | Int VB | 1i | – | 0.0 | – | 0.0 |
| | Ext VB/ Int WB | 1 | 0.0 (0.0) | 0.0 | 0.0 | 0.0 |
| | Ext WB | 2 | 0.0 (0.0) | – | – | 0.0 |
| | Air cavity | 3 | $0.1^{*0.002}$ (4.0) | $0.1^{*0.002}$ | 0.0 | $0.1^{*0.002}$ |

However, if the battens were in a more mould-robust material, leading to a medium-resistant layer, all four tests would result in a mould growth index below 0.1.

When examining the measured data for $HT_{Nuuk1[SE]}$, the risk for mould growth is only present around the wind barrier. However, according to the simulations, there is a minimal risk (less than 0.0) adjacent to the vapour barrier in the original construction (Test 4). In scenarios without a wind barrier, the mould index is zero at s1, but overall, the risk levels are similar for all membrane combinations.

With two exceptions, the indexes for the simulated constructions closely resemble those for the measured data. Firstly, s3 in the air cavity of $CLT_{Nuuk2[ESE]}$, the simulations are less exposed to risk than the measured data and secondly, s3 on the inner side of the wind barrier in $HT_{Nuuk1[SE]}$, where the situation is opposite. Implementing either a vapour membrane, a wind barrier, or both does not indicate that the mould risk could be decreased significantly.

## 4. Discussion

### 4.1. Results

The visualisations of the collected data presented in Fig. 5 and the RMSEs in Table 3 show that the models are of varying quality. Due to the similar construction types, orientations and years, the data can be used to assess the considered facades' robustness and durability. In some cases, the deviances can be justified with uncertainties. E.g., the errors for two independent façade constructions in Nuuk were generally highest in 2020, which might be caused by the reduced weather quality of the data from DMI for that specific year. In other cases, such connections are not identified, creating a foundation for discussing the façade performance. This section discusses the observations, while the uncertainties and limitations are addressed in Section 4.2.

Despite the close resemblance of the hygrothermal conditions in the two facades of $HT_{Nuuk1}$, slight variations were observed in the mould indexes presented in Fig. 6. In spring 2021, there was a temperature drop in the interior climate of $HT_{nuuk2[NW]}$, affecting the entire wall construction and causing the relative humidity to reach 100% in the air cavity. Comparing the two half-timber constructions ($HT_{Nuuk1}$ and $HT_{Nuuk2}$), it was found that the mould index was higher at s3 for $HT_{Nuuk2[NW]}$ than for the facades in $HT_{Nuuk1}$. On the other hand, $HT_{Nuuk2}$ exhibited the least critical mould index in the air cavity (s4). This discrepancy suggests that the temperature drop in the $HT_{nuuk2[NW]}$ construction might have contributed to the increased mould index.

#### *4.1.1. Mould indexes*

Mould indexes larger than 1 were found only on the exterior side of the wind barrier, as illustrated in Fig. 6. The air cavity is comparable to an outdoor environment, and mould outdoors is usually not considered a problem [51]. Consequently, the risk of indoor climate problems due to mould in this position remains low, even when the mould index is high. Thus, a threshold value of 2 may be too strict. However, mould in the air cavity might cause deterioration and reduced durability of the adjacent materials [51].

In the context of half-timber houses, the mould indexes observed in Sisimiut were generally lower than in comparable houses in Nuuk, suggesting that the climate in Nuuk is more conducive to mould problems than in Sisimiut. This finding is supported by the test pavilion study, where similar constructions were assessed and simulated for both climates [5]. The results were reversed for concrete façades. In $CON_{Nuuk[SSW]}$, the mould index in the air cavity was 6, while in Sisimiut, it remained below 1 in $CON_{sis[NNW]}$ and 2.4 in $CON_{sis[SSE]}$. As the interior climates and the constructions are very similar for the two concrete houses, the explanation must be found in the varying climates or the labour quality in the construction phase. These results also show that the concrete façades exposed to direct sunlight are at greater risk of mould growth.

Unfortunately, there were no CLT houses in Sisimiut to compare to the CLT houses in Nuuk. The two CLT houses in Nuuk performed differently, as $CLT_{Nuuk1}$ does not have any indexes above 0, while the air cavities in $CLT_{Nuuk2}$ oriented to the ESE and WNW measured 4 and above 5, respectively. As the façades of $CLT_{Nuuk1}$ were oriented towards NNW and SSE, it does not seem to relate to the orientations. A Norwegian study [51] found that the risk of mould growth in tall buildings was more related to the vertical sensor location than the orientation of the facades. In this study, however, the sensor placement was not considered.

The mould indexes in Fig. 6 and Table 4 showed that the presence of vapour and wind membranes did not significantly impact the risk of mould growth. A wind barrier can, however, increase airtightness and thus possibly reduce heat loss and increase surface temperatures. This finding is coherent with the findings in a Finnish study [7], identifying that it is safe to implement plastic vapour barriers in façades in cold climates. Unless the mould index of 2 should be a threshold value, even externally to a wind barrier, there is no indication of mould problems in any assessed construction type. Consequently, there is no ground for deeming any of the constructions unsuited for the Arctic climate; they all seem to have the needed robustness.

#### *4.1.2. Labour quality*

Despite the concluded robustness of the wall constructions, there is one more perspective to discuss: the importance of labour quality. The primary indicator of this problem is the concrete constructions, which are almost identical but relate very differently to the respective hygrothermal simulations and the risk of mould growth. They are located in different cities, and the one in Nuuk performs worse. The weather conditions in Fig. 3 show that the climate is colder in Sisimiut than in Nuuk, while the winds are often stronger in Nuuk than in Sisimiut. Thus, the issue seems to be related to the wind conditions. In the study of Vinha [6], focusing on external wind barriers, the labour quality and material choices were found essential to the airtightness of the constructions. Comparing the errors and hygrothermal conditions with the similar constructions evaluated in Ref. [5], it is clear that the constructions in this study perform worse than in a test facility meticulously constructed. This observation emphasises the essence of labour quality in the performance of the facades.

### *4.2. Limitations and uncertainties*

In a field study of this nature, numerous factors cause uncertainties. This section aims to outline those potentially affecting the results and imposing limitations to the study.

#### *4.2.1. Material properties*

As described in Section 2.1, the sensors, which measure the fundamental data for this study, were installed after the houses were built. Even though the responsible companies have provided building project information for this study, there are many unknown details about the implemented materials, possible last-minute solutions, and project changes. Most materials were only specified generally, such as “insulation” or “OSB-board”, which leaves an extensive range of material properties to fit the description. The lack of information is a significant uncertainty to the quality of the Delphin models, despite the attempt to account for it by calibrating the material properties through iterations.

#### *4.2.2. Model fitting and initial conditions*

When fitting the models, there are endless opportunities for adjustments. It creates uncertainty that the model is based on and fitted to exact data, as these could be unexpected or faulty due to, e.g., drifting sensors or inadequate construction work. Nevertheless, in this study, the property adjustments are made within realistic limits found in literature or datasheets. Conclusively, the comparison only reveals whether the hygrothermal conditions are realistic or likely to occur for the individual construction type.

The initial conditions were set to 20 °C and 50% RH for all models. It is an uncertainty with little impact on the RMSE because of the relatively short period (approximately two weeks) until equilibrium with the dynamic boundary conditions from the interior and exterior climates. It was found sufficiently precise for this purpose, though it can be eliminated by simulating for two continuous years.

#### *4.2.3. Sensors*

As described in Section 2.1.2, the sensors are positioned to measure the hygrothermal conditions on the side opposite the membranes. It implies that they record the conditions in the air or material adjacent to the membrane instead of those directly on the membrane surface. Acknowledging this uncertainty when comparing the Delphin model results with the measurements is essential. For future field studies, it is recommended to reorient the sensors to measure as close to the membrane as possible.

Another uncertainty regarding the sensors is their tendency to drift, particularly in humidity measurements. Ideally, the sensors should be removed from the buildings after data collection for calibration and adjustments for any discrepancies in the data. However, this process presents multiple disadvantages and challenges. Firstly, it would end all measurements, though the observations from future climatic phenomena might be valuable. Secondly, it is time-consuming and expensive, requiring labour to pull out the sensors and expenses for transportation and salary.

In the results of this study, only one indication of drift was observed, specifically in $HT_{sis2[SE]}$. The suspicion is based on the temperatures being higher on the exterior side of the vapour barrier than on the inside. However, there is a possible alternative explanation. The sensor datasheet [28] describes a margin of precision, meaning that if the two temperatures were relatively close, and the internal sensor measured lower while the external sensor measured at the higher end of the margin, this could cause the observed results.

*4.2.4. Evaluation method, RMSE*

There are endless ways to evaluate the quality of the models. Knowing the limitations and advantages is essential, regardless of the applied evaluation method. There are two primary advantages to using RMSE. First, it is easy to interpret once the success criteria are defined, as the unit matches the investigated parameter. Second, the error does not depend on the observation value, meaning that RMSE is equally sensitive to deviances at low and high values. The primary disadvantage of this evaluation method is the sensitivity to peaks and outliers, which can lead to high errors based on a few extreme data points [32]. This issue has been dealt with using 7-day moving mean values for relative humidity.

Despite the considerations for choosing RMSE as the evaluation method to ensure equal sensitivity to errors through the constructions, the errors were generally more significant in the exterior layers than close to the indoor climate. The bigger errors near the exterior climate might be caused by the many weather parameters, affecting the measured data and challenging the accuracy when simulating the hygrothermal wall conditions.

*4.2.5. Mould index and time frame*

The mould indexes were calculated for periods equivalent to the measured data. As time is a significant factor in the Viitanen model [48], the mould indexes might increase if analysed for a longer time frame. However, research by Ojanen et al. [47] shows that very low indexes, in this case, many are 0, are unlikely to increase significantly over an extended time frame. The study shows that susceptible materials can attain mould index 5 in just 20 weeks when exposed to critical conditions. As all mould risk assessments in this study considered a minimum of 52 weeks for materials classified as "very sensitive", the limited time ranges are not expected to impact the results significantly. Nonetheless, this perspective supports evaluating more sensitive materials to compensate for the limited time frames.

*4.2.6. Geography and climate*

This study is limited by the monitored houses being located in only two different cities, namely, Nuuk and Sisimiut. However, these locations are favourable since they represent significant proportions of the Greenlandic population, inhabiting more than 43% [24]. Still, when evaluating the suitability and robustness of the façade constructions for the overall Greenlandic climate, this restricted geographical scope must be considered a limitation.

In the previous study presenting data from the test pavilion [5], see Section 1.3, the same three construction types were analysed for five different Greenlandic climates using ERA5 weather files. Concerning mould growth risk, all constructions were concluded to be robust under varying conditions. However, the conditions in the pavilion differed from the houses because the pavilion had a controlled interior climate, and the walls were meticulously constructed under controlled conditions.

The applied climate data, especially in Sisimiut, cause uncertainties due to the production method of ERA5 weather [38]. The data from DMI has more missing data points, which also causes uncertainties. A previous study [5] found that similar Delphin simulations were insensitive to applying ERA5 weather data instead of locally measured data.

*4.2.7. Relation to a previous assessment of $CON_{Nuuk}$*

In this study, the robustness was evaluated based on the risk of mould growth. However, the façades may not perform as anticipated due to inadequate construction work. A previous study of $CON_{Nuuk}$ [12] concluded that the temperature between the insulation and concrete was lower than expected because of airflows through the insulation, see Section 1.3. It also concluded that it might be possible to eliminate this issue by implementing a wind barrier, reducing the risk of cold wind penetrating the unevenly installed insulation layer. This conclusion is supported by Ref. [5], considering a test facility with a similar construction but implemented with high accuracy and quality control, where the measured data was in line with the expected hygrothermal conditions created by simulations. This can explain why the simulations and measurements were consistent for $CON_{sis}$ and not $CON_{Nuuk}$.

## 4.3. Outlook

As the performance of a building is highly dependent on airtightness, the economic and environmental impact of a wind barrier might be a worthy trade-off to ensure the best quality and reduce the risk of having to redo parts of the façade. Thus, evaluating the consequences of excluding certain elements, such as the wind barrier, is recommended.

For further research, it is interesting to investigate why mould is prevalent in residential buildings despite this and other studies identifying low humidity levels and, consequently, reduced mould risks.

## 5. Conclusion

In this study, the hygrothermal data from 9 façade structures in Nuuk and Sisimiut were presented along with simulations representing the expected hygrothermal behaviours of the constructions. The ambition was to identify if the absence of wind barriers could cause hygrothermal issues. This study assessed two perspectives on this issue: mould and temperature. The mould indexes, presented in Fig. 6 and Table 4, showed that the risk of mould could not be eliminated by implementing a wind barrier.

Furthermore, the study intended to identify if all the represented constructions were robust to the Arctic climate. Again, this was evaluated based on the hygrothermal conditions and the risk of mould. When assessing the risk of mould growth, most of the constructions are at some risk in the outer layers, but only three half-timber constructions ($HT_{sis2}$, $HT_{Nuuk1}$, and $HT_{Nuuk2}$) are at risk on the inner side of the wind barrier. Furthermore, the values are so small that they will unlikely grow significantly over an extended period. Thus, the constructions can all be considered robust regarding mould. All assessed construction types have examples where the hygrothermal measurements and simulations align. However, there are also discrepant comparisons from both locations pointing toward the importance of fulfilling practical aspects.

## CRediT authorship contribution statement

**Naja Kastrup Friis:** Writing – review & editing, Writing – original draft, Visualization, Software, Methodology, Formal analysis, Data curation. **Eva B. Møller:** Writing – review & editing, Supervision, Methodology, Conceptualization. **Tove Lading:** Project administration, Funding acquisition, Conceptualization.

## Declaration of competing interest

The authors declare that they have no known competing financial interests or personal relationships that could have appeared to influence the work reported in this paper.

## Data availability

Data will be made available on request.

## Acknowledgements

This study was supported by DTU, DTU Byg, Grønlands Selvstyre, Kommunerqarfik Sermersooq, Greenland, Kernn-Jespersens Fond, A. P. Møllers Fond and Knud Højgaards Fond.

## References


[1] J.C. Madsen, Grønlandske Boliger - Selvbyggeri Og Typehuse, Forlaget Atuagkat, 2000.
[2] E.B. Møller, T. Lading, Current building strategies in Greenland, E3S Web Conf. 172 (2020), https://doi.org/10.1051/e3sconf/202017219004.
[3] Rigsarkivet, "Nuna-Tek/GTO [Online]. Available: https://www.sa.dk/daisy/arkivskaber_detaljer?a=&b=&c=&d=&e=&f=&g=&h=&ngid=407286&ngnid=&heid=&henid=&epid=&faid=&meid=&m2rid=&side=&sort=&dir=&gsc=&int=&ep=&es=&ed=.
[4] IAPP's Committee Regarding Test Constructions, Byggeriets effektivisering, 2002.
[5] N.K. Friis, E.B. Møller, T. Lading, Hygrothermal assessment of external walls in Arctic climates: field measurements and simulations of a test facility, Build. Environ. 238 (Jun. 2023), 110347, https://doi.org/10.1016/j.buildenv.2023.110347. February.
[6] J. Vinha, Hygrothermal Performance of Timber-Framed External Walls in Finnish Climatic Conditions: A Method for Determining the Sufficient Water Vapour Resistance of the Interior Lining of a Wall Assembly, 2007.
[7] J. Langmans, Feasibility of Exterior Air Barriers in Light Weight Construction, 2013.
[8] Technical University of Denmark, Om Projektet - ABC - Arctic Building and Construction, 2022 [Online]. Available: https://abc-byg.dtu.dk/om-projektet. (Accessed 5 May 2022).
[9] E.B. Møller, T. Lading, Preliminary assessment of the building design of a new test house in Nuuk, Greenland, J. Phys. Conf. Ser. 2069 (1) (2021) 1–4, https://doi.org/10.1088/1742-6596/2069/1/012228.
[10] A. Slyngborg, Study of Energy Performance and Optimization for Buildings in Greenland A Case Study of Prøvehuset in Nuuk for Potential Purposes, 2021.
[11] U. Andersen, DTU Advarer : Ny Byggemetode Giver Kuldeproblemer I Grønland, 2020, pp. 3–5.
[12] N.K. Friis, E.B. Møller, T. Lading, Can collected hygrothermal data illustrate observed thermal problems of the façade? - a case study from Greenland, J. Phys. Conf. Ser. 2069 (2021), https://doi.org/10.1088/1742-6596/2069/1/012071.
[13] L.M. Ottosen, Lavenergihuset I Sisimiut, 2006, pp. 1–2.
[14] Direktoratet for Boliger og Infrastruktur, Bygningsreglement, 2006, p. 158, 2006.
[15] S.R. Petersen, Pivutæt Grønlandsk Lavenergihus Når Ikke Egne Energimål, 2010. Ingeniøren.
[16] C. Rode, P. Vladykova, M. Kotol, Air Tightness and Energy Performance of an Arctic Low-Energy House, October, 2010.
[17] M. Kotol, Energy Use and Indoor Environment in New and Existing Dwellings in Arctic Climates, 2014.
[18] Vejrarkiv DMI [Online]. Available: https://www.dmi.dk/vejrarkiv/, 2020. (Accessed 16 December 2020).
[19] S. Ilomets, T. Kalamees, J. Vinha, Indoor hygrothermal loads for the deterministic and stochastic design of the building envelope for dwellings in cold climates, J. Build. Phys. 41 (6) (May 2018) 547–577, https://doi.org/10.1177/1744259117718442.
[20] E.B. Møller, J. Helgason, Weather and indoor climate in Greenland, J. Phys. Conf. Ser. 8 (2021).
[21] R.J. Stanborough, A. Cattamanchi, Dry Air: How Dry Air Can Affect Your Health, Plus Prevention Tips, Healthline, 2020 [Online]. Available: https://www.healthline.com/health/dry-air. (Accessed 23 February 2023).
[22] M. Kotol, C. Rode, G. Clausen, T.R. Nielsen, Indoor environment in bedrooms in 79 Greenlandic households, Build. Environ. 81 (2014) 29–36, https://doi.org/10.1016/j.buildenv.2014.05.016.
[23] R. Krishnan, et al., An influence of dew point temperature on the occurrence of Mycobacterium tuberculosis disease in Chennai, India, Sci. Rep. 12 (1) (2022) 1–10, https://doi.org/10.1038/s41598-022-10111-4.
[24] Statistics Greenland, Greenland in Figures 19 (2022) 36, 2022.
[25] AS Boligselskabet INI, Skimmelsvamp." [Online]. Available: http://www.byginfo.gl/media/1124/ini-as-skimmelsvamp.pdf.
[26] Baumklimatik-Dresden, DELPHIN," 2022. [Online]. Available: http://bauklimatik-dresden.de/delphin/index.php. (Accessed 23 January 2021).
[27] V. Kukk, A. Bella, J. Kers, T. Kalamees, Airtightness of cross-laminated timber envelopes: influence of moisture content, indoor humidity, orientation, and assembly, J. Build. Eng. 44 (April, 2021), https://doi.org/10.1016/j.jobe.2021.102610.
[28] Innovative Sensor Technology, "HYT 221 Digital Humidity and Temperature Module." p. 3.
[29] B. Hejari, N.R.M. Sakiyama, J. Frick, H. Garrecht, Hygrothermal Simulations Comparative Study : Assessment of Different Materials Using WUFI and DELPHIN Software Bina Hejazi, 2019, pp. 4674–4681. Nayara R . M . Sakiyama , Jürgen Frick , Harald Garrecht Materials Testing Institute (MPA), University of Stuttgart , Stuttgart.
[30] M. Defo, M. Lacasse, A. Laouadi, A comparison of hygrothermal simulation results derived from four simulation tools, J. Build. Phys. 45 (4) (2022) 432–456, https://doi.org/10.1177/1744259120988760.
[31] A. Tijskens, S. Roels, H. Janssen, Neural networks to predict the hygrothermal response of building components in a probabilistic framework, in: Healthy, Intelligent and Resilient Buildings and Urban Environments, 2018, pp. 1169–1174, https://doi.org/10.14305/ibpc.2018.ms-6.04. December 2019.
[32] V. Kukk, L. Kaljula, J. Kers, T. Kalamees, Designing highly insulated cross-laminated timber external walls in terms of hygrothermal performance: field measurements and simulations, Build. Environ. 212 (November 2021), 108805, https://doi.org/10.1016/j.buildenv.2022.108805, 2022.
[33] O. May Tzuc, et al., Modeling of hygrothermal behavior for green facade's concrete wall exposed to nordic climate using artificial intelligence and global sensitivity analysis, J. Build. Eng. 33 (July 2020) 2021, https://doi.org/10.1016/j.jobe.2020.101625.
[34] S. Vogelsang, H. Fechner, A. Nicolai, Delphin 6 Material File Specification, 2013, Version 6.0.
[35] P. Mukhopadhyaya, M.K. Kumaran, J. Lackey, N. Normandin, D. van Reenen, F. Tariku, Hygrothermal properties of exterior claddings, sheathing boards, membranes, and insulation materials for building envelope design, Therm. Perform. Exter. Envel. Whole Build. 1 (2007) 1–13.
[36] Cembrit, "Cembrit Multi Force," [Online]. Available: https://www.cembrit.dk/download/SDK/montagevejledninger/montagevejledning-cembrit-multi-force, 2017. (Accessed 31 January 2023).
[37] Cembrit, "Cembrit Windstopper [Online]. Available: https://www.cembrit.com/download/CHDK/datasheets/cembrit-windstopper-basic-datasheet, 2018.
[38] European Centre for Medium-Range Weather Forecasts, ERA5 | ECMWF, https://www.ecmwf.int/en/forecasts/datasets/reanalysis-datasets/era5, 2022. (Accessed 17 January 2023) [Online]. Available:.
[39] D.G. Erbs, S.A. Klein, J.A. Duffie, Estimation of the diffuse radiation fraction for hourly, daily and monthly-average global radiation, Sol. Energy 28 (4) (1982) 293–302, https://doi.org/10.1016/0038-092X(82)90302-4.
[40] J. Langmans, S. Roels, Experimental analysis of cavity ventilation behind rainscreen cladding systems: a comparison of four measuring techniques, Build. Environ. 87 (2015) 177–192, https://doi.org/10.1016/j.buildenv.2015.01.030.
[41] J. Falk, K. Sandin, Ventilated rainscreen cladding: measurements of cavity air velocities, estimation of air change rates and evaluation of driving forces, Build. Environ. 59 (2013) 164–176, https://doi.org/10.1016/j.buildenv.2012.08.017.
[42] G.M. Girma, F. Tariku, Experimental investigation of cavity air gap depth for enhanced thermal performance of ventilated rain-screen walls, Build. Environ. 194 (2021), 107710, https://doi.org/10.1016/j.buildenv.2021.107710. October 2020.
[43] J. Brozovsky, A. Nocente, P. Rüther, Modelling and validation of hygrothermal conditions in the air gap behind wood cladding and BIPV in the building envelope, Build. Environ. 228 (November 2022) (2023), 109917, https://doi.org/10.1016/j.buildenv.2022.109917.
[44] E. Brandt, et al., SBI-Anvisning 277, Fugt I Bygninger - Teori, Beregning Og Undersøgelse, vol. 1, BUILD, 2023.
[45] A. Hukka, H.A. Viitanen, A mathematical model of mould growth on wooden material, Wood Sci. Technol. 33 (6) (Dec. 1999) 475–485, https://doi.org/10.1007/s002260050131.
[46] Fraunhofer Institute for Building Physics, WUFI® Mould Index VTT, 2022 [Online]. Available: https://wufi.de/en/2017/03/31/wufi-mould-index-vtt/. (Accessed 26 January 2023).
[47] T. Ojanen, et al., Mold growth modeling of building structures using sensitivity classes of materials, in: ASHRAE Build. XI Conf. Dec. 5-9, 2010 Cleawater Beach, 2010. Florida.
[48] H. Viitanen, T. Ojanen, R. Peuhkuri, Mould growth modelling to evaluate durability of materials, Proc. 12DBMC - Int. Conf. Durab. Build. Mater. Components (2011) 1–8.
[49] N.K. Friis, E.B. Møller, Repository for Hygrothermal Conditions in the Facades of Residential Buildings in Nuuk and Sisimiut, 2023, https://doi.org/10.11583/DTU.22212103.
[50] R. Wang, H. Ge, D. Baril, Moisture-safe attic design in extremely cold climate: hygrothermal simulations, Build. Environ. 182 (2020), 107166, https://doi.org/10.1016/j.buildenv.2020.107166. July.
[51] S.B. Ingebretsen, E. Andenæs, L. Gullbrekken, T. Kvande, Microclimate and mould growth potential of air cavities in ventilated wooden façade and roof systems—case studies from Norway, Buildings 12 (10) (Oct. 2022) 1739, https://doi.org/10.3390/buildings12101739.